Appl Biochem Biotechnol (2009) 157:285–298
DOI 10.1007/s12010-008-8357-2

Autoacetylation of Purified Calreticulin Transacetylase Utilizing Acetoxycoumarin as the Acetyl Group Donor

Seema Bansal · Prija Ponnan · Hanumantharao G. Raj · Susan T. Weintraub · Madhu Chopra · Ranju Kumari · Daman Saluja · Ajit Kumar · Tapesh K. Tyagi · Prabhjot Singh · Ashok K. Prasad · Luciano Saso · Ramesh C. Rastogi · Virinder S. Parmar

Received: 17 February 2008 / Accepted: 26 August 2008 /
Published online: 16 September 2008

Abstract Our earlier reports documented that calreticulin, a multifunctional Ca^{2+}-binding protein in endoplasmic reticulum lumen, possessed protein acetyltransferase function termed Calreticulin Transacetylase (CRTAase). The autoacetylation of purified human placental CRTAase concomitant with the acetylation of receptor proteins by a model acetoxycoumarin, 7,8-Diacetoxy-4-methylcoumarin, was observed. Here, we have examined the autoacetylation property of CRTAase by immunoblotting and mass spectrometry. Ca^{2+} was found to inhibit CRTAase activity. The inhibition of both autoacetylation of CRTAase as well as acetylation of the receptor protein was apparent when Ca^{2+} was included in the reaction mixture as visualized by interaction with anti-acetyl lysine antibody. The acetylation of lysines residues: −48, −62, −64, −153, and −159 in N-domain and −206, −207, −209, and −238 in P-domain of CRTAase were located by high-performance liquid chromatography-electronspray ionization tandem mass spectrometry. Further, computer assisted protein structure modeling studies were undertaken to probe the effect of autoacetylation of CRTAase. Accordingly, the predicted CRTAase 3D model showed that all the loop regions of both N- and P-domain bear the acetylated lysines.

S. Bansal · P. Ponnan · H. G. Raj (✉) · R. Kumari · A. Kumar · T. K. Tyagi · P. Singh
Department of Biochemistry, V. P. Chest Institute, University of Delhi, Delhi 1100 07, India
e-mail: rajhg@yahoo.com

P. Ponnan · A. K. Prasad · R. C. Rastogi · V. S. Parmar
Department of Chemistry, University of Delhi, Delhi 1100 07, India

M. Chopra · D. Saluja
Dr.B.R.Ambedkar Center for Biomedical Research, University of Delhi, Delhi 1100 07 Delhi, India

S. T. Weintraub
Department of Biochemistry, The University of Texas Health Science Center, 7703 Floyd Curl Drive, San Antonio, TX 78229-3900, USA

L. Saso
Department of Human Physiology and Pharmacology,
"Vittorio Erspamer" Sapienza University of Rome, P.le Aldo Moro 5, 00185 Rome, Italy

Energy minimization of the acetylated residues revealed charge neutralization of lysines due to the N-ε-acetylation which may facilitate the interaction of CRTAase with the protein substrate and the subsequent transacetylase action.

Keywords Protein acetyltransferase · Calreticulin · Acetoxycoumarin · Protein acetylation · Mass spectrometry

Introduction

Calreticulin (CR) is one of the most important Ca^{2+}-binding proteins in the endoplasmic reticulum (ER) of eukaryotic cells. CR is divided into three structural and functional domains [1]. The amino terminal (N-domain) is highly conserved and binds Zn^{2+} with high capacity [2, 3]. It is followed by proline rich P-domain that binds Ca^{2+} with high affinity (K_d=0.05–10 μM and 1 mol of Ca^{2+}/mol of protein) [4]. The carboxy terminal (C-domain) is highly acidic bearing clusters of aspartate and glutamate residues, binds Ca^{2+} with high capacity (K_d=~1–2 mM and ~25–50 mol of Ca^{2+}/mol of protein) [4, 5]. CR in coordination with its paralog calnexin functions as molecular chaperones in the correct folding of nascent N-linked glycoproteins in the ER lumen [6]. Even though CR is a soluble ER protein and calnexin is type 1 ER membrane protein [1, 6], they are known to possess remarkable amino acid structural and sequence similarity. Peptide segments of these two homologous proteins have varying sequence identity ranging from 42–78% [7].

Recently the X-ray crystal structure of calnexin luminal domain from dog [8] and NMR solution structure of rat CR P-domain has been determined [9].

We have established the transfer of acetyl group from 7,8-Diacetoxy-4-methylcoumarin (DAMC), a model acetoxy drug to certain receptor proteins such as glutathione S-transferase (GST), nicotinamide adenine dinucleotide phosphate (NADPH) cytochrome P-450 reductase and nitric oxide synthase (NOS) [10–12]. In our recent report, we have provided mass spectrometric evidence for the placental CRTAase-mediated acetylation of nNOS by DAMC [13]. The analysis of protein acetylation by mass spectrometry has gained popularity because of its sensitivity and rapid characterization of post-translational modifications [14, 15].We observed the concomitant acetylation of CR during the CRTAase catalyzed reaction. Such autoacetylation of CR was investigated recently [13, 16]. In this study, electrospray ionization (ESI)-tandem mass spectrometry (MS/MS) was used to localize the acetylated residues within the sequence of human placental CRTAase. In order to visualize the acetylated sites, a theoretical three dimensional structure of CRTAase was predicted and the modified amino acids were analyzed with respect to the neighboring amino acid groups of the secondary structure of CRTAase.

Materials and Methods

Materials

Anti-acetyl lysine polyclonal antibody was purchased from Cell Signaling Technology, Beverly, MA, USA. Goat anti-rabbit horse radish peroxidase (HRP) conjugated secondary antibody and diaminobenzidine (DAB) were purchased from Bangalore Genei, Bangalore, India. Acryl amide, ammonium per sulphate, TEMED, bis-acrylamide, pre-stained molecular weight markers were purchased from BioRad, Hertfordshire, United Kingdom.

Glycine, Trizma base, sodium dodecyl sulphate (SDS), reduced glutathione (GSH), 1-chloro-2,4 dinitrobenzene (CDNB), EDTA, were procured from Sigma Chemicals Co., St. Louis, MO, USA. Standard molecular weight markers for SDS-PAGE were procured from MBI Fermentas. Modified trypsin was supplied by Promega, Madison, WI, USA. All other chemicals used were of high purity and were obtained from local suppliers.

Purification of CRTAase from Human Placenta

Placenta was obtained from Gauri Nursing Home, Malka Ganj, Delhi, India from healthy, 25–40-year-old patients who had no symptoms of any infectious disease. Placenta was stored and brought to the laboratory in an ice box within 30 min of delivery. Placental microsomes and cytosol were prepared as described earlier [16]. Protein content was estimated by the method of Lowry et al. [17]. Placental CRTAase was purified as described earlier [16]. For this purpose, microsomal pellet was solubilized by brief homogenization in 0.1M phosphate buffer, pH 7.4 and 5% sodium cholate using the method of Dey et al. with modifications [18]. The clear supernatant obtained after solubilization was dialyzed overnight against 10 mM potassium phosphate buffer (pH 7.4) containing 1 mM EDTA, 1 mM DTT, and 1 mM PMSF. The dialyzed fraction was subjected to CM-Sepharose, DEAE-Sepharose, and Q-Sepharose chromatographies to purify the protein to homogeneity.

Assay of CRTAase

CRTAase in placental microsomes was assayed routinely using DAMC as the first substrate (unless otherwise mentioned) and cytosolic GST as the second substrate, using the method of Raj et al. [12]. The percentage inhibition of cytosolic GST under the conditions of the assay was considered proportional to CRTAase activity.

SDS PAGE

Autoacetylation experiments were carried out using DAMC and the purified CRTAase [16], the production of acetylated CRTAase was quantified after separating the components of the reaction on sodium dodecyl sulfate polyacrylamide gel electrophoresis (SDS-PAGE). Appropriate controls were taken to elucidate the role of CRTAase in catalyzing the autoacetylation. Purified CRTAase was incubated with DAMC (100 μM), 10 mM phosphate buffer (pH 7.2) without any receptor protein and incubated for 30 min at 37 °C in a water bath. After the completion of the reaction, sample buffer (loading dye) was added to the reaction mixture to stop the reaction. This reaction mixture was loaded onto SDS-PAGE. The gel electrophoresis was carried out with discontinuous buffer system originally devised by Orstein [19] and Davis [20] followed by the procedure of Laemmli [21]. The samples and the stacking gel were prepared in Tris–HCl (pH 6.8). All components of the system contained 0.1% SDS.

Western Blot Analysis

For the detection of the acetylated lysine residues, western blot analysis was carried out using anti-acetyl lysine polyclonal antibody. The electrophoretically separated protein were transblotted to polyvinylidene fluoride (PVDF) membrane at 300 mA for 3 h at 4 °C. Non-specific sites on the PVDF were blocked with blocking reagent (5% Blotto). Primary

antibody dilution (1:1,000) was prepared in TBST (Tris-buffered saline (TBS) with 0.05% Tween) containing 1% BSA and incubation was carried out in 4 °C overnight with slight agitation.

The PVDF membrane was extensively washed with TBST. Goat anti-rabbit HRP conjugated secondary antibody approximately diluted in TBST was then added and incubation for 1 h at room temperature was carried out. The sheets were then washed extensively with TBST/TBS.

Acetylated protein was immunodetected with rabbit polyclonal anti-acetylated lysine (1:1,000) and developed with goat anti-rabbit IgG secondary antibody coupled to HRP using DAB system.

Effect of Calcium on CRTAase Catalyzed Acetylation of NADPH Cytochrome P-450 Reductase and Autoacetylation

In order to demonstrate the effect of calcium on CRTAase catalyzed acetylation of receptor protein, DAMC (100 μM) was separately preincubated with or without calcium (5 μM) along with the purified CRTAase (M. wt. 60 KDa) and receptor protein (NADPH cytochrome P-450 reductase) followed by western blot using anti-acetyl lysine antibody as described above. Appropriate controls having DMSO in place of DAMC and other one having no enzyme were taken. In the same manner, DAMC (100 μM) was preincubated with calcium (5 μM) followed by addition of CRTAase [16] to elucidate the role of calcium on autoacetylation.

In-Gel Protein Reduction

The acetylated bands were cut and placed in a 0.6-ml tube filled with ultra pure water. The bands were washed with 40 mM ammonium bicarbonate, 50% acetonitrile. Wash reagent, 500 μl, was added to each tube followed by slow inversion mixing for 10 min. The washing step was repeated and the tube was filled with acetonitrile. The band was allowed to incubate end over end for another 10 min. At this point, the bands were dehydrated piece of plastic. The acetonitrile was removed by spinning at 1,000 rpm for 5 min and the bands were ready for trypsin digestion.

HPLC-ESI-MS/MS

The excised bands were digested in situ with trypsin in 40 mM NH_4HCO_3 at 37 °C for 4 h. The digests were analyzed without further purification by capillary high-performance liquid chromatography (HPLC)-electrospray ionization tandem mass spectra (HPLC-ESI-MS/MS) acquired on a Thermo Fisher LTQ linear ion trap mass spectrometer (San Jose, CA, USA) fitted with a New Objective Pico View 550 nanospray interface. The source was coupled online to an Eksigent Nano LC micro HPLC (Dublin, CA, USA). The digest were dissolved in mobile phase A (0.5% acetic acid (HAc)/0.005% trifluroacetic acid (TFA)) and loaded onto a micro HPLC column PicoFrit™ (Woburn, MA, USA; 10 cm length × 75 μ i.d.) packed with C_{18} adsorbant (Vydac, Hesperia, CA; 218MS 5 μM particle size, 300 Å pore diameter). The peptides were eluted from the column with a gradient of 2% to 42% mobile phase B (90% acetonitrile/0.5% HAc/0.005% TFA) for 30 min with a flow rate of 0.4 μl/min. The eluted peptides were electrosprayed into the linear ion trap mass spectrometer (2.9 KV ESI voltage, three isolation window for MS/MS and 35% relative collision energy).

Mass Spectrometric Data Analysis

The spectrum were surveyed by scan strategy followed by acquisition of data-dependent collision-induced dissociation (CID) mode that determined seven most intense ions in the survey scan above a set threshold. The uninterpreted CID spectra were searched against the NCBI-nr database with MASCOT search engine (Matrix Science, London, UK) [22]. Methionine oxidation and lysine acetylation were considered as variable modification for all searches. Cross correlation of the Mascot results with X! Tandem [23] was done and determination of protein identity probabilities was accomplished by Scaffold™ (Proteome Software Inc.).

Molecular Modeling

Because the crystal structure of calreticulin has not been determined the effect of acetylation was investigated by computer-assisted modeling studies. The sequence of CR was obtained from Swiss-Prot database (Accession Number P27797). The crystal structure of mammalian calnexin (PDB entry 1JHN) [8] provided the major template needed for modeling the structure of two domains (viz. P and N-domain) of CR. The solution structure of CR P-domain (PDB entry 1HHN) [9] was used as other template for modeling P-domain. Also X-ray crystal structure of ten amino acid signal peptide sequence of CR complexed with class I MHC was used (PDB entry 2CLR) [24] to model the N-terminal region. ClustalW, automatic sequence alignment tool available at the website http://www.ebi.aa.uk/ was used for the initial alignment of the amino acid sequence. The default parameter corresponding to penalty of 10 for gap opening, 0.05 for gap extension and 8 for gap separation was assigned to the alignment [25]. The alignment was further corrected as against the structurally conserved regions of the potential templates (Fig. 1) using InsightII/ Homology [26]. The Modeller module within InsightII software suite [26] was then utilized

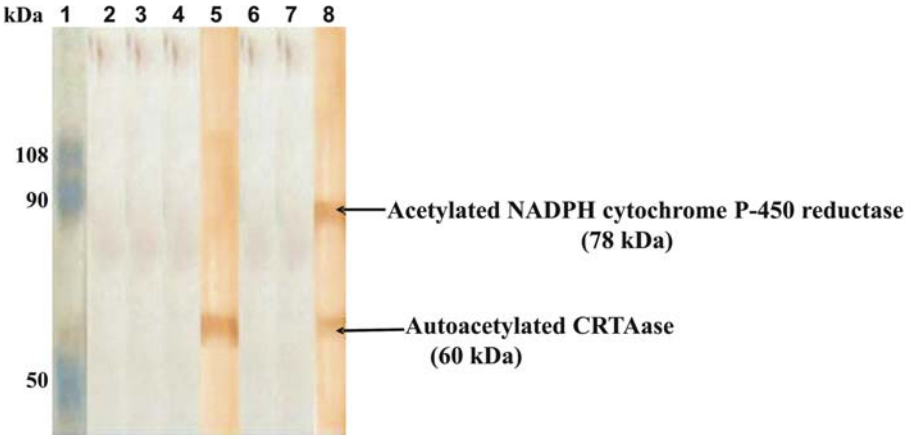

Fig. 1 Sequences of calnexin (PDB ID 1JHN), CR P-domain (PDB ID 1HHN), CR signal peptide sequence (PDB ID 2CLR) and human CR sequence swissprot accession no. P27797 are aligned using InsightII/ Homology and displayed by BOXSHADE program (http://www.ch.embnet.org/software/BOX_form.html). Shaded residues denote identity (*Black*) or close similarity (*Gray*) between sequences

to assign coordinates to regions structurally aligned to template, build intervening loops, optimize the rotamers of amino acid side chains and perform an initial energy optimization of the structure. The disulfide bond in CR N-domain (Cys105-Cys137) which is conserved in calnexin (Cys161-Cys195) was assigned to the initial model as predicted by homology with calnexin.

Biopolymer module implemented in InsightII [26] was used to modify lysines −48, −62, −64, −153, −159, −206, −207, −209, and −238 by the addition of an acetyl group, from the InsightII fragment library, to the side chain N-ε-atom. Using the same module, hydrogen atoms were added to the acetylated and non-acetylated protein structures at pH 7.0. The default consistent valence force field (cvff) force field [27] was applied to both the structures, the net charge of resulting protonated state of the acetylated protein was −68 and non-acetylated protein was −59. Further, a series of energy minimization steps were performed on both the protein structures by InsightII/Discover [26] using following protocol: (a) In the first step of minimization, all the heavy (all non-hydrogen) atoms were constrained, the hydrogen atoms were allowed to minimize using 100 cycles of steepest decent until the maximum derivative (|dE/dr|) of the system was <1 kcal/(mole Å). (b) This step was followed by another steepest descent minimization with the same parameter as in step (a), but constraining the protein backbone atoms and relaxing all other atoms of the molecule. (c) In the final step, the protein molecule was minimized using 50 cycles of conjugate gradient method with the backbone atom fixed and allowing all other atoms relax until the maximum derivative was <0.01 kcal/(mole Å). The final RMS derivative for both the minimized structure was found to be <0.001. The difference in the interaction after N-ε atom modifications of lysine residues were analyzed by InsightII [26].

Results

We have earlier documented isolation, purification, and characterization of CRTAase from human placental microsomes [16]. The placental CRTAase was found to have molecular weight of 60 kDa and exhibited differential specificities to various classes of polyphenolic acetates. Placental CRTAase was incubated with a receptor protein NADPH cytochrome P-450 reductase and DAMC followed by western blot analysis using anti-acetyl lysine antibody. CRTAase when preincubated with $CaCl_2$ (3 μM) was found to be inhibited [16]. These observations bring home the influence of Ca^{2+}-binding site on CRTAase activity.

Effect of Calcium on CRTAase Catalyzed Acetylation of NADPH Cytochrome P-450 Reductase

The controls where $CaCl_2$ (5 μM) was not added showed the bands of acetylated proteins (78 kDa corresponding to the molecular weight of NADPH cytochrome P-450 reductase, Fig. 2; lane 8) and 60 kDa corresponding to the autoacetylated CRTAase (Fig. 2; lane 5, 8) as visualized by the anti-acetyl lysine antibody. CRTAase catalyzed acetylation of NADPH cytochrome P450 reductase by DAMC was found to be abolished in presence of Ca^{2+} (Fig. 2; lane 7). The autoacetylation of CRTAase was also found to be inhibited in the presence of $CaCl_2$ (5 μM) (Fig. 2; lane 6). The abolishment of CRTAase activity due to calcium resulted in the disappearance of autoacetylation of CRTAase as well as acetylation of receptor protein. These results advocated that the catalytic activity of CRTAase was essential for its autoacetylation by DAMC (Fig. 2; lane 5–8).

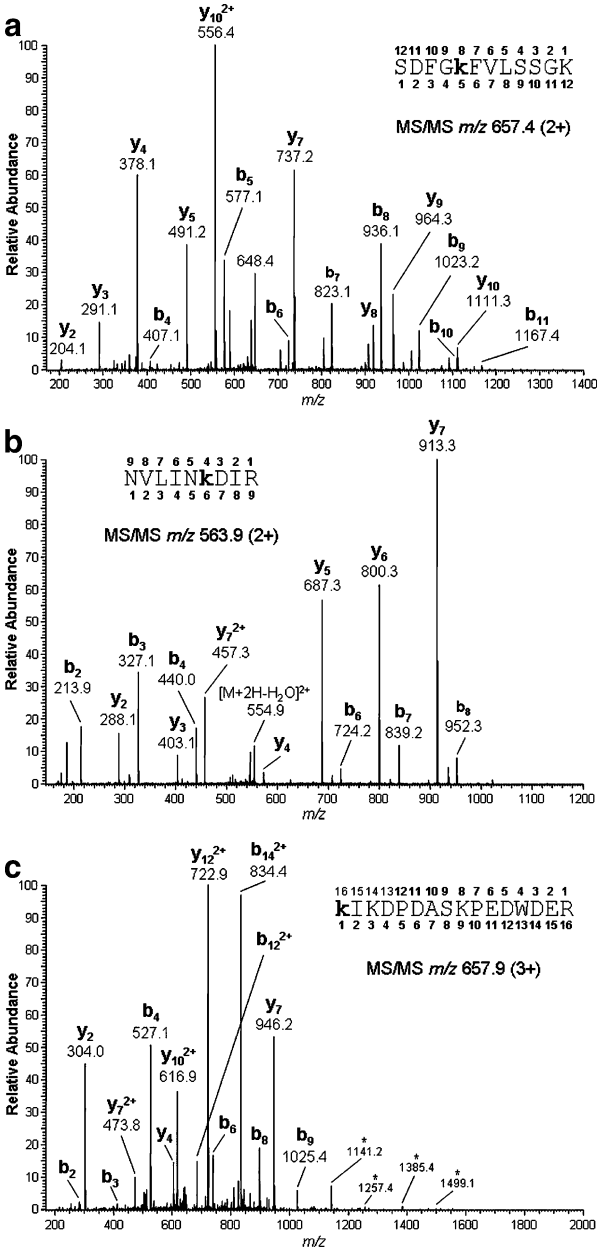

Fig. 2 Effect of Ca^{2+} on CRTAase catalyzed acetylation of NADPH cytochrome P-450 reductase by DAMC. Lane *1* Prestained molecular weight markers; lane *2* CRTAase+DMSO; lane *3* NADPH cytochrome P-450 reductase+DAMC; lane *4* CRTAase+DMSO+$CaCl_2$+(5 μM)+NADPH cytochrome P-450 reductase; lane *5* CRTAase+DAMC; lane *6* CRTAase+$CaCl_2$+(5 μM)+DAMC; lane *7* CRTAase+$CaCl_2$+(5 μM)+DAMC+NADPH cytochrome P-450 reductase; lane *8* CRTAase+DAMC+NADPH cytochrome P-450 reductase

ESI-MS/MS

The results from ESI-MS/MS revealed the localization of acetylated lysines of autoacetylated CRTAase. For this purpose, the CRTAase was incubated with DAMC for 30 min as described under "Materials and Methods" section. The reaction mixture was subjected to SDS-PAGE for the separation of autoacetylated CRTAase. The autoacetylated

CRTAase so obtained was devoid of any contaminating proteins and was considered suitable for MS analysis. In order to confirm autoacetylation of CRTAase and locate the possible acetylation sites, the protein was in-gel digested with trypsin and resulting peptide mixture was subjected to ESI-MS/MS analysis. The CID spectra obtained analyzed by the proteome search engines MASCOT and X! Tandem [22, 23], indicated 18 distinct peptides with a significant score as acetylated on lysine residues. Further the peptides identified by the two search engines were statistically validated by Scaffold software (Proteome Software Inc.) as highlighted in Table 1. These results confirmed the identity of acetylated tryptic peptides from human CR bearing nine acetylated lysine residues, Lys −48, −62, −64, −153, −159, −206, −207, −209, and −238.

The CID spectra were obtained for all the nine peptides, three of them are shown in Fig. 3a–c. In the CID spectrum of tryptic peptide corresponding to CR $^{44–55}$ at m/z 657.4 (2+), the acetylation of Lys-48 is confirmed by b5 and y8 ions (Fig. 3a). Similarly in the CID spectrum of the tryptic peptide corresponding to CR$^{154–162}$ at m/z 563.9 (2+), acetylation of Lys-159 is confirmed by b6 and y4 ions (Fig. 3b).

Molecular Modeling

The predicted 3D model of calreticulin (Fig. 4) contains the main structural characteristics of calreticulin: an N-terminal globular domain, the central P-domain "extended hairpin-like

Table 1 Acetylated peptides detected in the tryptic digest of autoacetylated CRTAase.

Sequence	Probability	Mascot ion score	X! Tandem score	Modifications	Residues
(K)EQFLDGDGWTSR(W)	95%	73.42	6.80		25–36
(K)SDFG**k**FVLSSGK(F)	95%	74.14	2.70	Acetyl (+42)	44–55
(K)FVLSSGK(F)	95%	37.72	2.00		49–55
(K)FYGDEEKDKGLQTSQDAR(F)	95%	46.48	4.20		56–73
(K)FYGDEE**k**DKGLQTSQDAR(F)	95%	54.08	4.47	Acetyl (+42)	56–73
(K)FYGDEEKD**k**GLQTSQDAR(F)	95%	61.27		Acetyl (+42)	56–73
(K)G**k**NVLINK(D)	95%	49.39	3.00	Acetyl (+42)	152–159
(K)NVLIN**k**DIR(C)	95%	45.86	1.96	Acetyl (+42)	154–162
(K)IDNSQVESGSLEDDWDFLPPKK(I)	95%	67.59	5.82		186–207
(K)IDNSQVESGSLEDDWDFLPP**k**K(I)	95%	55.59	5.15	Acetyl (+42)	186–207
(K)IDNSQVESGSLEDDWDFLPPK(K)	95%	135.14	7.68		186–206
(K)**k**IKDPDASKPEDWDER(A)	95%	44.45	3.09	Acetyl (+42)	207–222
(K)**k**I**k**DPDASKPEDWDER(A)	95%		2.77	Acetyl (+42), Acetyl (+42)	207–222
(K)IKDPDASKPEDWDER(A)	95%	39.95	2.55		208–222
(R)AKIDDPTDSKPEDWD**k**PEHIPD PDAK(K)	95%	63.97	5.85	Acetyl (+42)	223–248
(K)IDDPTDSKPEDWD**k**PEHIP DPDAK(K)	95%		4.31	Acetyl (+42)	225–248
(K)KPEDWDEEMDGEWEPPVI QNPEYK(G)	95%	58.11	7.35		249–272
(K)KPEDWDEE**m**DGEWEPPVI QNPEYK(G)	95%	68.83	5.44	Oxidation (+16)	249–272

Purified placental CRTAase was incubated with DAMC, the modified protein was separated on the SDS-PAGE, digested with trypsin at 37° for 4 h and processed for analysis by LC-MS/MS. Tryptic peptides are identified by Scaffold software (Proteome Software Inc.) with significant Mascot and X! Tandem score

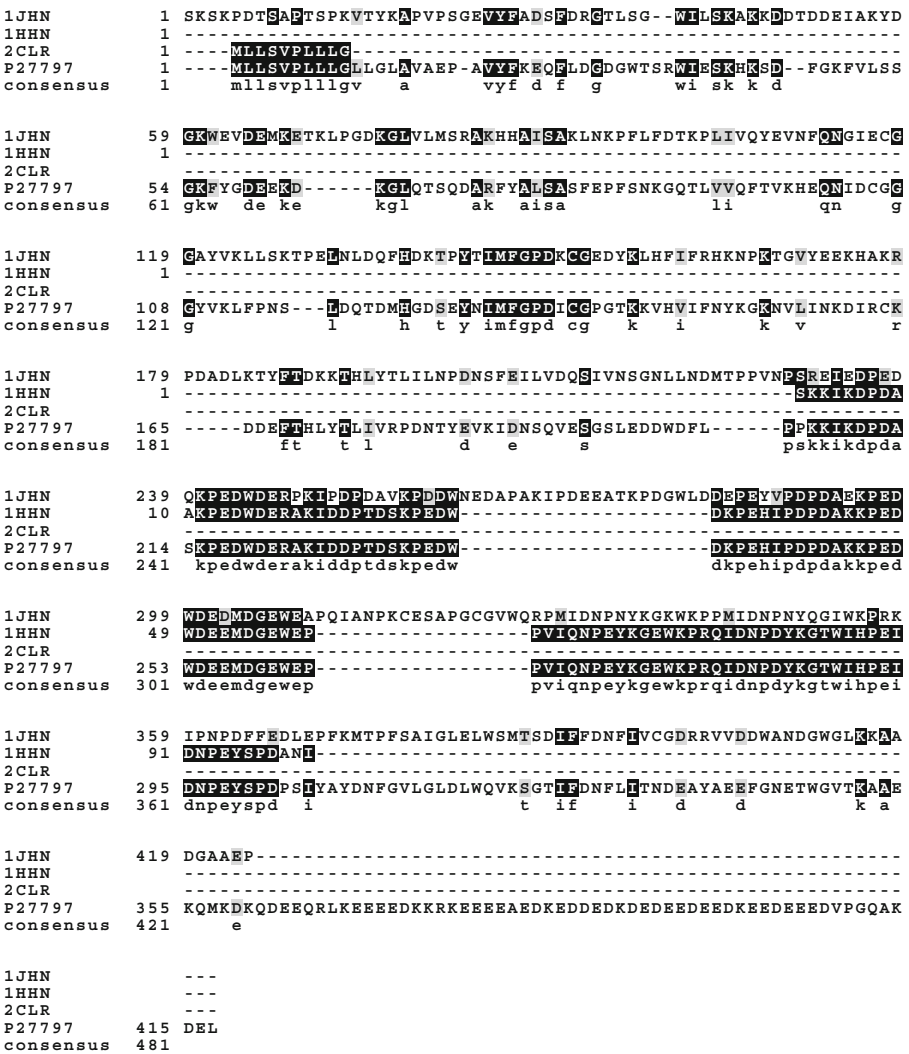

Fig. 3 Tandem mass spectra of selected CR tryptic peptides containing acetyl-lysine. Residue numbers shown in *boldface* type above and below the peptide sequences indicate detected collision-induced dissociation fragments for y-series (C-terminal) and b-series (N-terminal) ions, respectively. **a** Sequence SDFG**k**FVLSSGK (Corresponding to residues 45–55 of CR) observed in the tryptic digest of CR, the ion at m/z 648.4 was generated by loss of water from doubly charged precursor; **b** sequence NVLIN**k**DIR (Corresponding to residues 154–162 of CR) peak at m/z 554.9 represents the ion due to loss of water in the doubly charged precursor; **c** sequence **k**IKDPDASKPEDWDER (Corresponding to residues 207–222 of CR) observed in the tryptic digest of CR. MS/MS m/z 657.9 (3+). *Asterisk* corresponds to internal fragments

arm" comprising the two types of repeated motifs PXXIXDPDAXKPEDWDE (type 1) and GXWXPPXIXNPXYX (type 2) arranged in 111222 fashion and the C-terminal domain bearing clusters of aspartate and glutamate residues. The modeling study provided us to analyze the localization of acetylated lysine residues in the 3D structure of CR. All the acetylated lysine residues located by LC-MS/MS were visualized in the N- and P-domain of CR (Fig. 4). The predicted 3D structure of CR revealed that the five acetylated lysines in

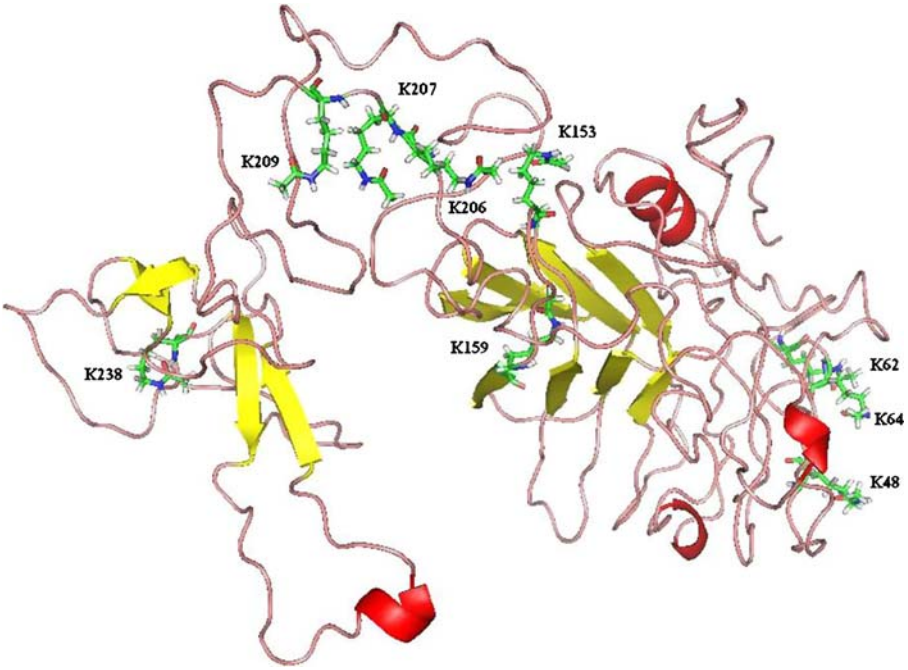

Fig. 4 The predicted structure of CR is represented in Kabsch–Sander secondary structure with α-helices in *red* and β-sheets in *yellow*. The modified lysine residues are in stick representation with standard atom colors. The figure was prepared using Pymol software [43]

the N-domain (Lys −48, −62, −64, −153, and −159) were found to be in the exposed surface of the protein. Similar trend was observed in the case of the four acetylated lysines of P-domain (Lys −206, −207, −209, and −238). To examine effect of acetylated residues on enzyme stability, energy minimization calculations were performed on the modeled structure CR bearing acetyl group. The interactions of lysine residues with neighboring amino acid side chains and backbone atoms were explored. Examination of all the energetic state of protein by different rounds of energy minimization have evidenced that in most cases of the acetylated CR, a loss of H-bonds of the ε-amino group lysine residues and acidic counterparts such as aspartate and glutamate residues as observed in comparison with non-acetylated form (Figs. 5 and 6). This is due to the loss of positive charges on the specific lysine residues owing to acetylation and thus failing their ability to form intermolecular H-bonds with the aspartate and glutamate residues.

Discussion

Our earlier studies proposed the concept of enzymatic acetylation of protein independent of acetyl CoA. The ER was shown to contain a unique enzyme TAase, as described in our earlier reports [11, 12], catalyzing the transfer of acetyl group to certain functional proteins. TAase was purified to homogeneity from human placental microsomes and exhibited M. wt. of 60 kDa. The N-terminal sequence of purified TAase was found to exhibit 100% identity with N-terminal sequence of mature CR [28]. The identity of TAase with CR was further confirmed from the properties of CR such as immunoreactivity with anti-CR,

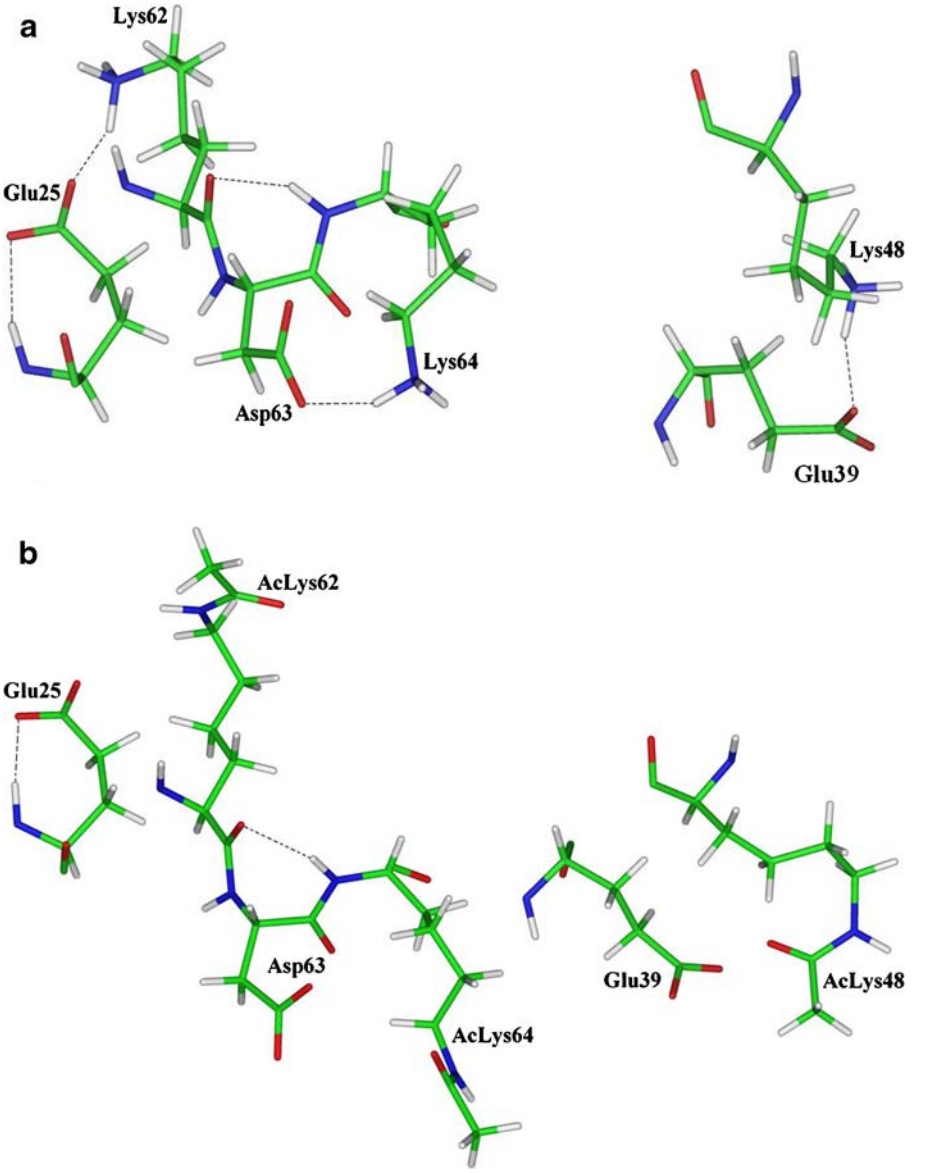

Fig. 5 Comparison of intermolecular H-bonds (*dotted lines*) of lysines with glutamate and aspartate residues in non-acetylated (**a**) and acetylated (**b**) CR, after energy minimization. The amino acid residues are rendered in *sticks with standard atom colors*. Loss of H-bonds between Lys-62 and Glu-25, Lys-64 and Asp-63 also in Lys-48 and Glu-39 was observed due to neutralization of the positively charged lysine residue by acetylation. The acetylated lysine residues of N-domain are *highlighted* here. The figure was generated using InsightII program [26]

Ca^{2+}-binding and being a substrate for protein kinase [16]. We have in this communication made the efforts to establish the transacetylase-dependent acetylation of CR utilizing acetoxycoumarins as the acetyl group donors. CR is one of the major Ca^{2+}-binding proteins in the ER. Studies show that binding of Ca^{2+} to calreticulin appears to induce

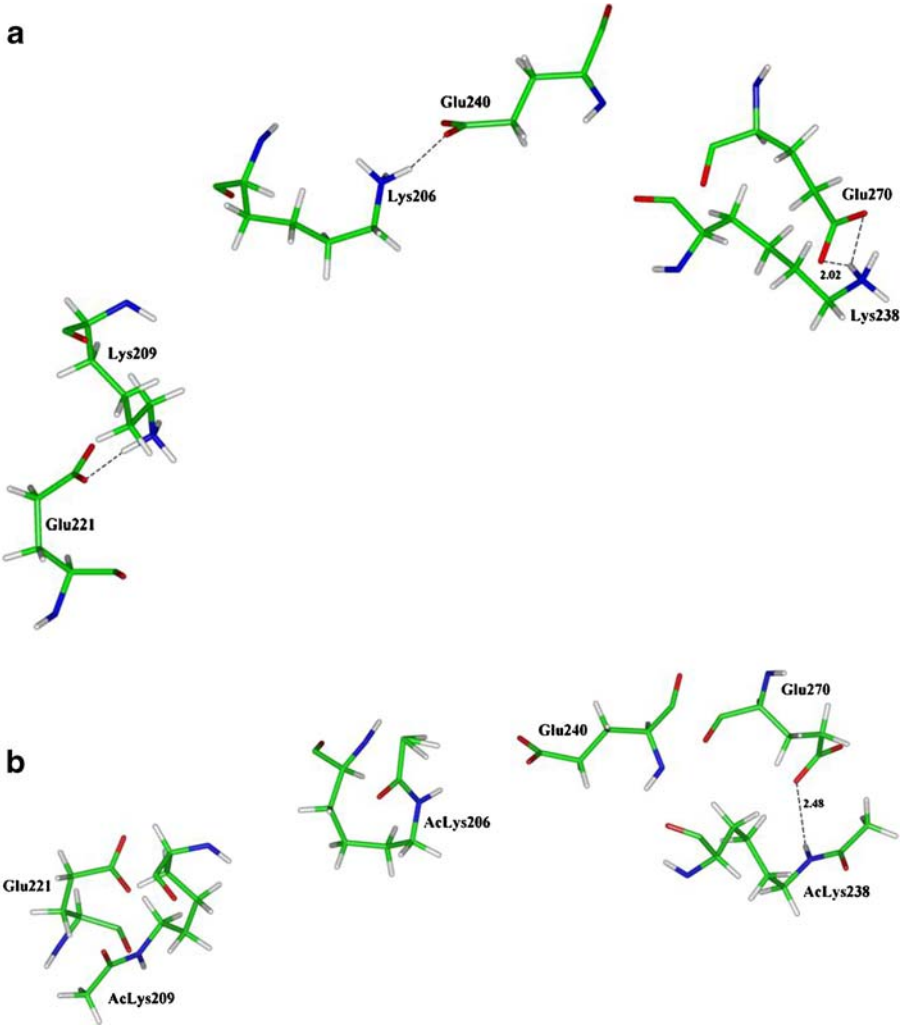

Fig. 6 Comparison of non-acetylated (**a**) and acetylated (**b**) CR P-domain lysines. Loss of H-bonds between Lys-206 and Glu-240, Lys-238 and Glu-270 as well as Lys-209 and Glu-221 was observed due to *N*-ε-acetylation of lysine residues. Also, increase in the intermolecular distances between acetyl-lysine (AcLys-238) and glutamate (Glu-270) is observed. The amino acid residues are rendered in *sticks with standard atom colors*. The amino acid residues rendered in sticks with standard atom colors and figure is realized using InsightII program [26]

conformational change in the protein and shown to modulate the activities of CR by forming a core which is resistant to proteolysis. Also this ion-induced conformational change is accountable for Ca^{2+}-dependent interaction of CR with PDI and ERP57 [29]. The inhibition of autoacetylation of CR by Ca^{2+} as recorded here may be viewed in this context.

Mass spectrometric analysis located five acetylated lysine residues in N-domain (Lys −48, −62, −64, −153, and −159) and four acetylated lysine residue in P-domain (Lys −206, −207, −209, and −238) of CR, one methionine (Met-257) oxidation is also observed. Computer-assisted modeling of CR revealed lysines in the loop region of these two domains getting covalently modified (Fig. 4). None of the lysine residues in the C-domain

was observed to be covalently modified by acetylation. The effect of covalent modification N-ε-acetyl-lysine was analyzed by the energy minimization studies. Several rounds of energy minimization revealed neutralization of lysine residue and breaking of intermolecular H-bond with neighboring acidic residues (Figs. 5 and 6). These effects of modification by way of acetylation of lysine residues could facilitate interaction of CR with other proteins.

Cellular protein acetylation is mediated by the prototype of histone acetyltransferases (HAT). Several classes of HAT, nuclear (Type A) as well as cytosolic (Type B), are known to exist. Gcn5/PCAF, MYST and p300/CBP are the major examples of nuclear HAT and HAT1 is termed cytoplasmic HAT [30, 31]. Although, these enzymes catalyze protein acetylation by acetyl CoA, a number of distinct features among them are recognized in the case of nuclear HAT [32]. A few of such distinguishing features include sequence divergence and some HAT is found to acetylate non-histone proteins such as transcription factors p53 and MyoD [33, 34]. Lately, the existence of protein acetyltransferase in the ER lumen is reported [35]. Our recent studies conclusively established protein acetylation mediated by purified CR [13, 16, 28]. CR lacked any structural or sequence resemblances to prototypes of HAT. In this context, transcription factor IIB (TFIIB) could be cited as an example of protein acetyltransferase distinct from the HAT family. CR could be similar to TFIIB which is also known to undergo autoacetylation [36]. The results described in this paper have shown that the intact transacetylase function is necessary for the autoacetylation of CR (Fig. 2). There are reports of self-acetylated intermediate involving cysteine acetylation in the action of HAT (such as ESA1) activity [37]. Some experimental evidence highlights autoacetylation of HAT as in the case of the action of p300 [38] and TFIIB [36] where acetylated lysine is an intermediate. CRTAase was also found to be an acetyl CoA-linked protein acetyltransferase (unpublished data). The acetylated CR residue (LYS-206) is reported in certain cases of acute myeloid leukemia due to cytogenetic abnormalities, as analyzed by mass spectrometric studies. Also, the prognostic importance of the acetylation of lysine residue of CR has been highlighted [39]. It is pertinent to point out that the CR autoacetylation by DAMC in vitro has also resulted in the acetylation of Lys-206. Certain acetyltransferase mediated lysine acetylation is found to be abundant among mitochondrial proteins [40, 41]. Many energy metabolic pathway proteins and dehydrogenases were the key proteins being acetylated in mitochondria but the exact functions of acetylation are still unclear. Also, the proteomics survey carried out by Zhao and co-workers has highlighted the possible importance of lysine acetylation of many regulatory proteins including chaperones such as heat shock proteins, cyclophilin A, as well as other chaperones, subunits of TCP1 ring complex, and FK506-binding protein 4 [42]. Even the calcium-binding proteins are no exception with reports of Annexin V (a calcium-dependent phospholipids-binding protein) getting acetylated [42]. Accordingly, this investigation by the integrated approach of bioinformatics method and proteomic experiments can be perceived to interpret the significant biological consequence by autoacetylation of CR.

Acknowledgement This work was supported by Department of Biotechnology, Government of India and Italian Ministry of University and Research, General Management of Strategies and Development of Internationalization of Scientific and Technological Research.

References

1. Michalak, M., Milner, R. E., Burns, K., & Opas, M. (1992). *Biochemical Journal*, *285*, 681–692.
2. Khanna, N. C., Tokuda, M., & Waisman, D. M. (1986). *Journal of Biological Chemistry*, *261*, 8883–8887.

3. Baksh, S., Spamer, C., Heilmann, C., & Michalak, M. (1995). *FEBS Letters*, *375*, 53–57.
4. Baksh, S., & Michalak, M. (1991). *Journal of Biological Chemistry*, *266*, 458–465.
5. Treves, S., DeMattei, M., Lanfredi, M., Villa, A., Green, N. M., MacLennan, D. H., et al. (1990). *Biochemical Journal*, *271*, 473–480.
6. Williams, D. B. (1995). *Biochemistry and Cell Biology*, *73*, 123–132.
7. Wada, I., Rindress, D., Cameron, P. H., Ou, W. J., Doherty, J. J., Louvard, D., et al. (1991). *Journal of Biological Chemistry*, *266*, 19599–19610.
8. Schrag, J. D., Bergeron, J. J., Li, Y., Borisova, S., Hahn, M., Thomas, D. Y., et al. (2001). *Molecular Cell*, *8*, 633–644.
9. Ellgaard, L., Riek, R., Herrmann, T., Güntert, P., Braun, D., Helenius, A., et al. (2001). *Procedings of National Acadamy of Sciences of United States of America*, *98*, 3133–3138.
10. Khurana, P., Kumari, R., Vohra, P., Kumar, A., Seema, Gupta, G., et al. (2006). *Bioorganic and Medicinal Chemistry*, *14*, 575–583.
11. Raj, H. G., Parmar, V. S., Jain, S. C., Goel, S., Singh, A., Gupta, K., et al. (1999). *Bioorganic and Medicinal Chemistry*, *7*, 369–373.
12. Raj, H. G., Parmar, V. S., Jain, S. C., Kohli, E., Ahmad, N., et al. (2000). *Bioorganic and Medicinal Chemistry*, *8*, 1707–1712.
13. Bansal, S., Gaspari, M., Raj, H. G., Cuda, G., Verheij, E., Tyagi, Y. K., et al. (2008). *Applied Biochemistry and Biotechnology*, *144*, 37–45.
14. Dormeyer, W., Ott, M., & Scnolzer, M. (2005). *Molecular and Cellular Proteomics*, *4*, 1226–1239.
15. Kim, J. Y., Kim, K. W., Kwon, H. J., Lee, D. W., & Yoo, J. S. (2002). *Analytical Chemistry*, *74*, 5443–5449.
16. Seema, Kumari, R., Gupta, G., Saluja, D., Kumar, A., Goel, S., et al. (2007). *Cellular Biochemistry and Biophysics*, *47*, 53–64.
17. Lowry, O. H., Rosebrough, N. J., Farr, A. L., & Randall, R. J. (1951). *Journal of Biological Chemistry*, *193*, 265–275.
18. Dey, A. C., Rahal, S., Rimsay, R. L., & Senciall, I. R. (1981). *Analytical Biochemitry*, *110*, 373–379.
19. Ornstein, L. (1964). *Annals of New York Academy of Sciences*, *121*, 321–349.
20. Davis, B. J. (1964). *Annals of New York Academy of Sciences*, *121*, 404–427.
21. Laemmli, U. K. (1970). *Nature (London)*, *227*, 680–685.
22. Perkins, D., Pappin, D., Creasy, D., & Cottrell, J. (1999). *Electrophoresis*, *20*, 3551–3567.
23. Craig, R., & Beavis, R. (2004). *Bioinformatics*, *20*, 1466–1467.
24. Collins, E. J., Garboczi, D. N., & Wiley, D. C. (1994). *Nature*, *371*, 626–629.
25. Higgins, D., Thompson, J., Gibson, T., Thompson, J. D., Higgins, D. G., & Gibson, T. J. (1994). *Nucleic Acids Research*, *22*, 4673–4680.
26. InsightII, Version 2000 ed; Accelrys Inc.,: San Diego, CA.
27. Dauber-Osguthorpe, P., Roberts, V. A., Osguthorpe, D. J., Wolff, J., Genest, M., & Hagler, A. T. (1988). *Proteins: Structure, Function and Genetics*, *4*, 31–47.
28. Raj, H. G., Kumari, R., Seema, Gupta, G., Kumar, R., Saluja, D., et al. (2006). *Pure Applied Chemistry*, *78*, 985–992.
29. Elaine, F. C., Karolina, M. M., Kim, O., Steve, J., Iain, D. C., Paul, E., et al. (2000). *Journal of Biological Chemistry*, *275*, 27177–27185.
30. Ruiz-Carillo, A. B., Sendra, R., Galiana, M., Pamblanco, M., Perez-Ortin, J. E., & Tordera, V. (1998). *Journal of Biological Chemistry*, *273*, 12599–12605.
31. Marmorstein, R. (2001). *Cellular and Molecular Life Sciences*, *58*, 693–703.
32. Sterner, D. E., & Berger, S. L. (2000). *Microbiology and Molecular Biology Reviews*, *64*, 435–459.
33. Glozak, M. A., Sengupta, N., Zhang, X., & Seto, E. (2005). *Gene*, *363*, 15–23.
34. Zhang, K., & Dent, S. Y. (2005). *Journal of Cellular Biochemistry*, *96*, 1137–1148.
35. Costantini, C., Ko, M. H., Jonas, M. C., & Puglielli, L. (2007). *Biochemical Journal*, *407*, 383–395.
36. Chu, H. C., Makoto, H., & Anny, U. (2003). *Nature*, *424*, 965–969.
37. Yan, Y., Harper, S., Speicher, D. W., & Marmorstein, R. (2002). *Nature (Structural Biology)*, *9*, 862–869.
38. Thompson, P. R., Wang, D., Wang, L., Fulco, M., Pediconi, N., Zhang, D., et al. (2004). *Nature (Structural and Molecular Biology)*, *11*, 308–315.
39. Balkhi, M. Y., Trivedi, A. K., Geletu, M., Christopeit, M., Bohlander, S. K., Behre, H. M., et al. (2006). *Nature (Oncogene)*, *25*, 7041–7058.
40. Mootha, V. K., Bunkenborg, J., Olsen, J. V., Hjerrild, M., Wisniewski, J. R., Stahl, E., et al. (2003). *Cell*, *115*, 629–640.
41. Taylor, S. W., Fahy, E., Zhang, B., Glenn, G. M., Warnock, D. E., Wiley, S., et al. (2003). *Nature (Biotechnology)*, *21*, 281–286.
42. Sung, C. K., Robert, S., Yue, C., Yingda, X., Haydn, B., Jimin, P., et al. (2006). *Molecular Cell*, *23*, 607–618.
43. The PyMOL Molecular Graphics System, version 0.99; DeLano Scientific: San Carlos, CA, USA, 2002